Applied Catalysis B: Environmental 152–153 (2014) 397–402

Contents lists available at ScienceDirect

Applied Catalysis B: Environmental

journal homepage: www.elsevier.com/locate/apcatb

Promotion of Pt surfaces for ethanol electro-oxidation by the addition of small SnO_2 nanoparticles: Activity and mechanism

Joseph W. Magee [a], Wei-Ping Zhou [b], Michael G. White [a,b,*]

[a] Department of Chemistry, Stony Brook University, Stony Brook, NY 11974, United States
[b] Chemistry Department, Brookhaven National Laboratory, Upton, NY 11973, United States

ARTICLE INFO

Article history:
Received 22 November 2013
Received in revised form 18 January 2014
Accepted 28 January 2014
Available online 5 February 2014

Keywords:
Ethanol oxidation
SnO_2 nanoparticles
Pt surface
In situ IRRAS
Bi-functional catalyst

ABSTRACT

The catalytic effect of a SnO_2 co-catalyst for ethanol electrooxidation on polycrystalline Pt is studied by electrochemical methods, *in situ* infrared reflection-absorption spectroscopy, and high resolution transmission electron microscopy. The electrochemical results show that deposition of small SnO_2 NPs onto the pc-Pt electrode surface significantly enhances the catalytic performance of Pt. Infrared spectroscopy measurements show the effect that small SnO_2 particles have on the removal of CO from the Pt surface and suggest that the electrocatalytic C–C bond splitting activity of Pt, the key step in full conversion of ethanol to CO_2, is not affected by the addition of the –OH species provided by the SnO_2 particles. Also, it is shown that controlled deposition of SnO_2 is needed in order to control the rate of partial oxidation to acetic acid compared to full oxidation to CO_2. The combined results provide new insight into the role of SnO_2 co-catalysts in promoting the electro-oxidation of ethanol to CO_2 on Pt surfaces.

1. Introduction

Ethanol is attractive for fuel cell applications considering its availability from renewable sources, high energy density and low environmental impact as compared with other liquid fuels such as methanol and formic acid [1]. However, the slow kinetics and inefficient conversion of ethanol to CO_2 at low temperatures and low potentials hinder its wide-spread application. The complete oxidation of an ethanol molecule to CO_2 involves many elementary reaction steps, including C–C bond splitting, water activation to form –OH, and the oxidation of CO and CH_x intermediates into CO_2 [2–4]. Although Pt surfaces with low coordination sites are able to split the C-C bond [2–10], Pt alone is not an efficient catalyst for the ethanol oxidation reaction (EOR). This is due to the formation of strongly bound CO and CH_x intermediates, which poison Pt surfaces at low potentials [2,7–9]. Extensive efforts have been undertaken to identify and understand co-catalyst materials that can alleviate CO poisoning of Pt catalysts and improve the overall reaction kinetics.

Platinum-based catalysts promoted by the addition of tin oxides have been reported to have higher reactivity for the EOR compared to Pt itself [11–16]. Previous studies on mixed Pt/tin oxide powder samples using *in situ* infrared spectroscopy and differential electrochemical mass spectroscopy (DEMS) were able to detect reaction intermediates and products such as CO, CO_2, acetaldehyde and acetic acid [13–16]. However, the complexity of these Pt/SnO_2 binary nanocatalysts has led to some controversy regarding the nature of the active phase and the origin of their high EOR activity. For example, the enhanced EOR activity has been generally assigned to a bi-functional mechanism wherein the SnO_2 promotes water dissociation at low potentials, which enhances the oxidative removal of chemisorbed CO_{ads} at nearby Pt sites [13–16]. Measurements used to test this hypothesis are complicated by the presence of a Pt-Sn metallic alloy phase, often found in Pt/SnO_2 powders, which influences EOR activity and selectivity in a way that is different from Pt/SnO_2 interface sites [15,17–21]. In addition, the strong dependence of catalytic performance of Pt/SnO_2 powder catalysts on synthetic methods and activation conditions further impedes a clear understanding of the catalytic effect of SnO_2 co-catalysts in ethanol oxidation.

We have recently demonstrated that the deposition of SnO_2 nanoparticles (NPs) on planar Pt surfaces can be used as models of complex Pt/SnO_2 binary powder catalysts to investigate the chemical properties of SnO_2 and Pt/SnO_2 interface sites for electro-oxidation of methanol and ethanol [22,23]. Specifically, our studies showed that small SnO_2 NPs (~2 nm) deposited on a polycrystalline Pt (pc-Pt) electrode strongly enhance catalytic performance for methanol oxidation, while larger NPs (~20 nm) show a negligibly small promoting effect [22]. Prior to electrochemical measurements, x-ray photoelectron spectroscopy (XPS) measurements show that both small and large SnO_2 NPs are dominated by

* Corresponding author at: Stony Brook University, Department of Chemistry, Stony Brook, NY 11974, United States. Tel.: +1 631 3444345.
E-mail addresses: jmagee@bnl.gov (J.W. Magee), wpzhou@bnl.gov (W.-P. Zhou), mgwhite@bnl.gov (M.G. White).

0926-3373/$ – see front matter © 2014 Elsevier B.V. All rights reserved.
http://dx.doi.org/10.1016/j.apcatb.2014.01.057

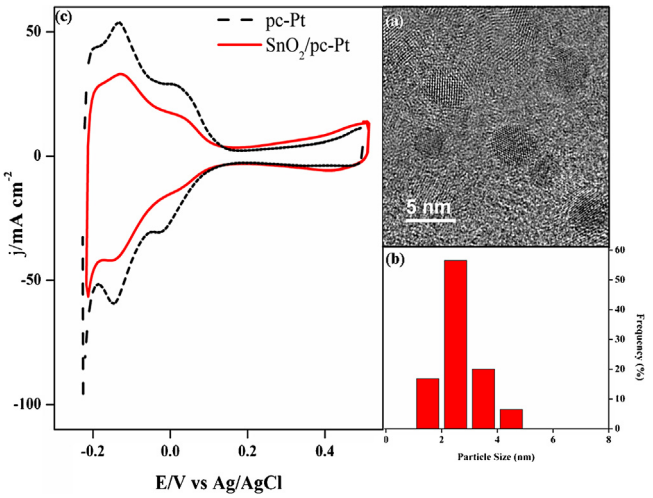

Fig. 1. (a) TEM image of SnO_2 deposited onto a pc-Pt electrode; (b) corresponding particle size distribution; (c) comparison of voltammetric curves for 2 nm SnO_2 NPs supported on pc-Pt and bare pc-Pt in 0.1 M $HClO_4$ solution. Scan rate: 50 mV/s. Currents in the present work are normalized to the bare Pt surface area (H_{upd} charge after double layer correction), prior to SnO_2 deposition, assuming a relationship of 210 μC/cm$^2_{pt}$.

Sn(IV) species. Interestingly, post-electrochemical reaction studies detected reduced Sn(II) species on SnO_2/Pt surfaces with ~2 nm SnO_2 NPs, but not with 20 nm NPs [22]. The enhanced activity was attributed to the presence of reduced Sn(II) species in small SnO_2 NPs [22].

In the present work, we use a model SnO_2/pc-Pt catalyst to investigate the catalytic effect of SnO_2 in the EOR. Catalytic activity, reaction mechanism and surface morphology are studied by a combination of electrochemical methods and *in situ* infrared reflection-absorption spectroscopy (IRRAS). The electrochemical measurements clearly demonstrate that the deposition of small (~2 nm) SnO_2 NPs on a pc-Pt electrode significantly enhances the EOR reactivity of Pt. The *in situ* IRRAS study provides mechanistic information on the catalytic role of SnO_2 NPs, as well as a comparison of the product distribution and selectivity of bare pc-Pt and SnO_2/pc-Pt surfaces. The insights gained from these results are expected to have important implications for further development of SnO_2/Pt based electrocatalysts for ethanol electooxidation.

2. Experimental

2.1. Preparation of SnO_2 (NPs)/pc-Pt electrode

0.25 mmol $SnCl_2{\cdot}2H_2O$ (99.99%, Sigma Aldrich) was dissolved in 4 ml ethylene glycol (Sigma Aldrich, 99.8%). This solution was then injected into a three-neck round bottom flask with 6 ml ethylene glycol that was pre-heated to 190 °C. High-purity water (Nanopure, Thermo Scientific) was added to the mixture to give a ratio of water to ethylene glycol of ~0.02. The solution was then refluxed at 190 °C and vigorously stirred in air for 40 min to obtain tin oxide NPs [11]. The tin oxide colloid was immediately quenched in an ice-water bath after reaction. Fig. 1a and b shows the HRTEM image of the SnO_2 NPs and the corresponding size distribution, respectively, indicating an average particle size of ~2 nm.

The freshly-prepared tin oxide NPs dispersed in ethylene glycol were sonicated for *ca.* 15 min before being deposited on a cylindrical polycrystalline Pt electrode. In a typical procedure, the electrochemical surface area (ECSA) and roughness factor of the Pt electrode was first determined in 0.1 M $HClO_4$ solution. Then, a certain volume of the tin oxide solution (20 μl for the present work) was pippetted onto the pc-Pt electrode surface. After precipitation in air for several hours, the tin oxide covered Pt electrode was dipped into 1.0 M NaOH and then ultra-pure water to remove residues such as ethylene glycol and Cl^- ions. The as-prepared electrode was then cycled in a blank solution followed by ethanol activity measurements in a different cell. In order to prevent SnO_2 dissolution and maintain its promotional effect, the potential is not cycled beyond 0.5 V. Right after the activity testing, the Pt electrode, partially covered with ~2 nm tin oxide NPs, was transferred into a three-electrode Teflon cell for IRRAS measurements.

2.2. Electrochemical measurements

All electrochemical experiments were performed at room temperature in a 0.1 M $HClO_4$ solution made with UHP H_2O and using an Autolab 128N potentiostat. An Ag/AgCl (sat. Cl^-) electrode (Bio) was used as the reference electrode. Currents in the present work are normalized to the bare Pt surface area using the H_{upd} charge after double layer correction assuming a value of 210 μC/cm$^2_{Pt}$. Prior to each electrochemical measurement, the solution was purged with argon gas for at least 30 min to remove dissolved oxygen.

2.3. IRRAS measurements

IR spectra were acquired using a Bruker Vertex 80V spectrometer equipped with a mid-band MCT detector at a spectral resolution of 4 cm^{-1}. The IRRAS cell utilizes a commercially available Teflon spectroelectrochemical cell (VeeMaxII, Pike Technologies) modified to accommodate 3 electrodes and an Ar purge line. A CaF_2 window was used to allow for IR transmission. Transmission was still >20% at 900 cm^{-1}. The polycrystalline Pt working electrode was pressed against the window to create a thin solution layer with a thickness of a few micrometers. A Pt foil and a leak-free Ag/AgCl electrode were used as the counter and reference electrode, respectively. The sample compartment was purged with Ar prior to IR measurements in order to remove spectral interference from CO_2 and water vapor in air. Initially the potential was held at −0.2 V *vs.* Ag/AgCl for 195 s, while a background scan was collected and used as the reference for all sample spectra. The potential was then stepped in the positive direction in 50 mV increments. A total of 128 single channel spectra were collected and averaged. Three scans were collected at each potential, 3 min apart, yielding a total time held at each potential of ~ 450 s. Spectra are given in absorbance units defined as $A = -\log(R/R_0)$, where R and R_0 represent the reflected IR intensities corresponding to the sample and reference-single beam spectrum, respectively.

3. Results and discussion

Fig. 1c compares the cyclic voltammagrams (CV) of a pc-Pt electrode partially covered with SnO_2 NPs with a bare pc-Pt electrode in 0.1 M $HClO_4$ solution. Deposition of SnO_2 NPs on the Pt electrode decreases the available Pt surface sites and we estimate a ~45% loss of Pt surface area from the change in H-desorption charge. The SnO_2/pc-Pt electrode shows stable CV features with continuous cycling up to 0.5 V.

Fig. 2a compares polarization curves for ethanol oxidation over the SnO_2/pc-Pt electrode and the bare pc-Pt electrode in a 0.5 M ethanol in 0.1 M $HClO_4$ solution at room temperature. Deposition of SnO_2 NPs on the pc-Pt electrode results in an active surface for the EOR that exhibits a large negative shift in the onset potential (~0.17 V) and a significantly higher current compared to the bare pc-Pt electrode. Chronoamperometric measurements shown in Fig. 2b confirm the enhancement in catalytic performance and stability for the SnO_2/pc-Pt electrode. After running the reaction for 1600 s at a potential of 0.20 V at room temperature, the SnO_2/pc-Pt

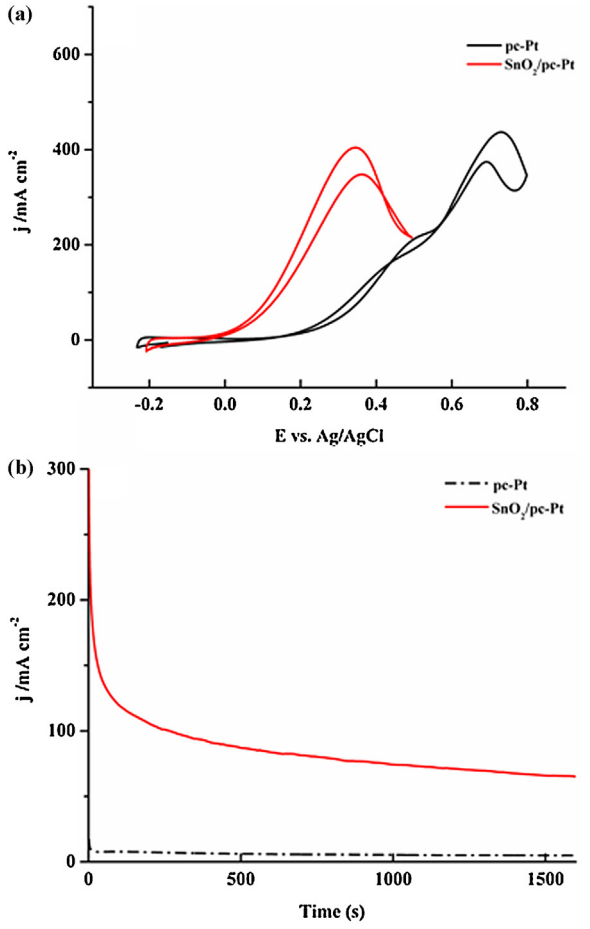

Fig. 2. (a) Comparison of current-potential polarization curves for a pc-Pt electrode decorated with SnO_2 NPs (red line) and a bare Pt electrode (black line) in 0.5 M ethanol and 0.1 M $HClO_4$ solution. Sweep rate is 10 mV/s. (b) Comparison of current-time plots for ethanol oxidation activity on the pc-Pt electrode with SnO_2 NP's (red) and a bare pc-Pt electrode (black) in a ethanol solution at 0.20 V for 1600 s reaction time at room temperature. (For interpretation of the references to color in this figure legend, the reader is referred to the web version of this article.)

electrode still exhibited high activity, with a measured current density of ~65 μA/cm^2. This is more than a 10–fold increase in current density compared with the bare pc-Pt electrode (5 μA/cm^2).

In situ IRRAS measurements were carried out to investigate the surface intermediates and product distribution for the potentiodynamic oxidation of ethanol on the SnO_2/pc-Pt and bare Pt electrodes. Fig. 3 shows IRRAS spectra at applied potentials in a 0.5 M ethanol in 0.1 M $HClO_4$ solution in the range of 2500–2000 cm^{-1} for both bare (a) pc-Pt and (b) SnO_2/pc-Pt. The band centered around 2050 cm^{-1} can be assigned to linear bound CO_{ads} on Pt, indicating that C–C bond cleavage of adsorbed ethanol has occurred. As the potential is swept towards more positive potentials a peak appears near 2343 cm^{-1}, which can be assigned to the asymmetric stretching vibration of CO_2 in solution; this CO_2 is the product of the complete oxidation of ethanol. Similarly, the wavenumber region 1350–850 cm^{-1} is shown in Fig. 4. The bands at 1280 cm^{-1} and 933 cm^{-1} are characteristic features of acetic acid and acetaldehyde, the main partial oxidation products, in solution. The spectral region 1150–1025 cm^{-1} contains two peaks. The peak that increases with potential at 1110 cm^{-1} is attributed to the adsorption of ClO_4^- while the peak at 1045 cm^{-1} is assigned to the C–O stretch of ethanol.

Although carbon monoxide, carbon dioxide and acetic acid are the main species observed on both SnO_2/pc-Pt and pc-Pt electrodes, their changes in intensity with potential are different. Fig. 5a shows a comparison of integrated intensities for the vibrational bands for CO_2 (~2343 cm^{-1}) and CO (~2050 cm^{-1}) plotted as a function of electrode potential. Similar data for acetic acid (~1280 cm^{-1}) and acetaldehyde (933 cm^{-1}) are shown in Fig. 5b. For the pc-Pt electrode, the band intensity of CO_{ads} is negligible at −0.2 V and increases with potential to a maximum at 0.25–0.3 V, and then drops down to almost zero at 0.55 V. This dependence of the CO_{ads} vibrational band on applied potential is in good agreement with previous studies of ethanol oxidation on pc-Pt electrodes by FTIR [8,9], SFG [2], and ATR-SEIRAS [7]. The observation of the CO_{ads} band clearly indicates that there are Pt active sites on the pc-Pt electrode capable of breaking the ethanol C–C bond.

Although the general trends of the intensity profiles for the CO_{ads} and CO_2 bands are similar for the SnO_2/pc-Pt and bare pc-Pt electrodes, there are two distinct differences. First, we note that the CO_{ads} band intensity begins to decrease at 0.15 V on SnO_2/pc-Pt, which is ~0.15 V lower than that on the bare Pt electrode and coincident with the appearance of the CO_2 band (Fig. 5a). This negative potential shift in the maximum CO_{ads} band intensity is a clear indication of the catalytic effect of the SnO_2 NPs for the EOR on Pt. The promoting effect of small SnO_2 NPs is associated with oxidative removal of CO_{ads} on Pt sites, and is consistent with our previous study of the MOR on a SnO_2/pc-Pt electrode [22]. Second, we note from Fig. 5a that the overall band intensity of CO_{ads} on the SnO_2/pc-Pt surface is about ~45% lower than that on the bare pc-Pt electrode, which is quite close to the loss of Pt surface area obtained from cyclic voltammetry (Fig. 1). Hence, the reduction of Pt surface sites on the SnO_2/pc-Pt electrode appears to have a negligible effect on CO_2 formation. The larger CO_2 integrated band intensity for the SnO_2/pc-Pt surface suggests that CO_2 formation is enhanced even though the available Pt surface has been reduced by SnO_2 particle deposition.

Addition of SnO_2 NPs on the Pt surface not only facilitates the complete oxidation of ethanol to CO_2, but also increases the production of acetaldehyde and acetic acid as evidenced by the IR bands at 933 cm^{-1} and 1280 cm^{-1}, respectively. Fig. 5b shows that the integrated band intensities for acetic acid and acetaldehyde are considerably larger on the SnO_2/pc-Pt electrode than the bare pc-Pt electrode. Noticeably, the onset potential (~0.15 V) of acetic acid formation occurs coincidently with the decrease of the CO_{ads} band and the appearance of the CO_2 product band. These observations suggest that SnO_2 NPs enhance both complete (CO_2) and incomplete (acetaldehyde/acetic acid) oxidation pathways for EOR on Pt. Since C–C bond breaking is expected to occur on Pt sites, the decrease in Pt surface area (~45%) on the SnO_2/pc-Pt electrode may result in a relatively larger accumulation of C_2 intermediates which then undergo facile oxidation at SnO_2/Pt interfaces.

In a second *in situ* IRRAS measurement, a constant potential of 0.2 V was applied and IRRAS spectra were followed with reaction time in an attempt to better understand the chronoamperometric measurements (Fig. 2). Static thin-layer studies are subject to mass transport limitations, which may promote the re-adsorption of intermediates and further oxidation, and the appearance of pH and diffusion gradients over time, which may alter product distribution [24]. However, identical experimental conditions should still allow for a meaningful comparison to be made between pc-Pt and SnO_2/pc-Pt product distribution over time. The integrated band intensities corresponding to the formation of CO_{ads}, CO_2 and acetic acid with reaction time are presented in Fig. 6. A negligible change with polarization time for the CO, CO_2 and acetic acid bands was observed on the pc-Pt electrode at 0.2 V. Since the highest coverage of CO_{ads} is also near 0.2 V (see Fig. 5a), the pc-Pt surface is therefore completely blocked for further ethanol adsorption and oxidation, consistent with the negligible current observed in the CA measurement (Fig. 2b). By contrast, the CO_2 and acetic acid band intensities with polarization

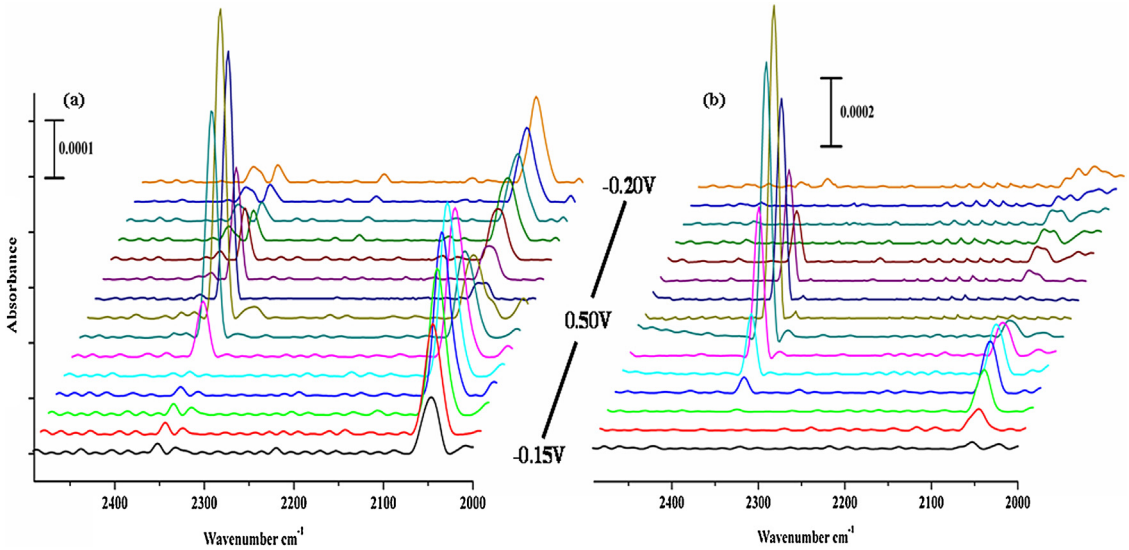

Fig. 3. *In situ* IRRAS spectra in the range 2500–2000 cm^{-1} recorded during ethanol electrooxidation in 0.5 M ethanol in 0.1 M $HClO_4$ solution: (a) a bare Pt electrode; (b) a SnO_2/pc-Pt electrode. Reference spectrum was taken at a potential of −0.20 V.

time on the SnO_2/pc-Pt electrode show completely different behavior. Most importantly, the CO_2 band intensity steadily increases with polarization time but the CO_{ads} band intensity remains constant (Fig. 5a). This is a clear indication that complete oxidation of ethanol to CO_2 occurs at 0.2 V on the SnO_2/pc-Pt electrode. However, partial oxidation of ethanol is also occurring at this potential as evident from the even larger increase in band intensity for acetic acid.

Numerous studies have shown that C–C bond splitting can occur on Pt surfaces at low applied potentials [2–9,25,26]. Density functional theory (DFT) calculations also suggest that there are no large barriers in the pathways leading to CO_{ads} and acetic acid formation [10]. However, further oxidation of CO_{ads} and $CH_{x,ads}$ is hindered at potentials relevant to fuel cells, where water dissociation on Pt is difficult [2,7,9]. Therefore, the chemisorbed CO and CH_x intermediates accumulate on the surface and block the Pt surface sites for ethanol adsorption and oxidation, as confirmed by our IRRAS measurement. Adding SnO_2 NPs as a co-catalyst on the pc-Pt surface leads to significantly enhanced activity and is assigned to the facile oxidation of CO_{ads} at low potentials (Figs. 4 and 5), which is related to the relative ease of water dissociation on SnO_2 NPs to form oxidizing –OH species. However, introducing –OH species to the Pt surface also increases the partial oxidation products (acetic acid and acetaldehyde), which leads to higher current densities, but lower selectivity and efficiency to CO_2.

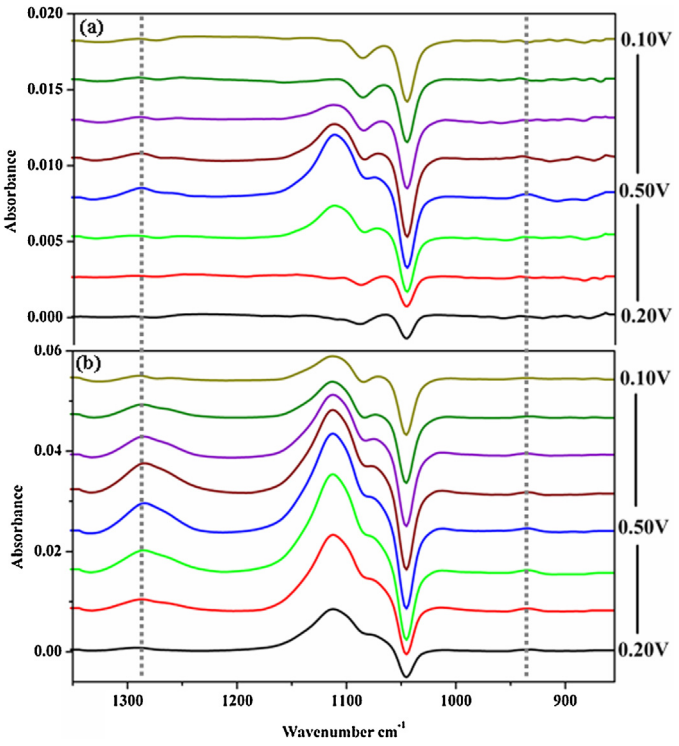

Fig. 4. *In situ* IRRAS spectra in the range 1350–850 cm^{-1} recorded during ethanol electrooxidation in 0.5 M ethanol in 0.1 M $HClO_4$ solution: (a) bare Pt electrode; (b) SnO_2/pc-Pt electrode. Reference spectrum was taken at a potential of −0.20 V.

Recently, Kavanagh et al., reported DFT calculation results for ethanol oxidation on a bare Pt surface with and without the presence of OH species [10]. They suggested that the formation of OH species on the Pt surface leads to a considerably increased reaction barrier for C–C bond splitting and hence inhibits CO_{ads} formation and CO_2 production. For the SnO_2/pc-Pt binary system, less available Pt sites for ethanol adsorption and reaction leads to a reduced formation of CO_{ads} (Fig. 3b). Interestingly, an increase, rather than a decrease in the CO_2 formation is observed in the entire potential region, including at potentials where the CO_{ads} can be oxidized at the bare Pt surface. Therefore, we believe that the Pt active sites on the SnO_2/pc-Pt electrode are not affected by the OH species at nearby SnO_2 sites and retain their ability to catalyze the full oxidation of ethanol. The data presented here, however, do not specifically address the effects of SnO_2 NPs on the oxidation of adsorbed CH_x intermediates, which could be an important issue for the complete oxidation of ethanol on SnO_2/Pt(1 1 1) surfaces [26,27].

Given that acetic acid formation also involves surface OH species *via* the reaction $CH_3CO + OH \rightarrow CH_3COOH$ [10], it is likely that the availability of OH species at SnO_2-Pt interface sites also decreases the reaction barrier and thereby increases its production rate. Since ethanol oxidation has been shown to have a strong dependence on the Pt surface structure [2–10], a controlled deposition of a SnO_2 co-catalyst that avoids covering Pt sites active for C–C bond splitting is likely to improve ethanol conversion to CO_2. In this regard, Del Colle et al. [26] demonstrated that the electrochemical deposition of Sn on Pt step sites on a Pt(3 3 2) surface increases acetic

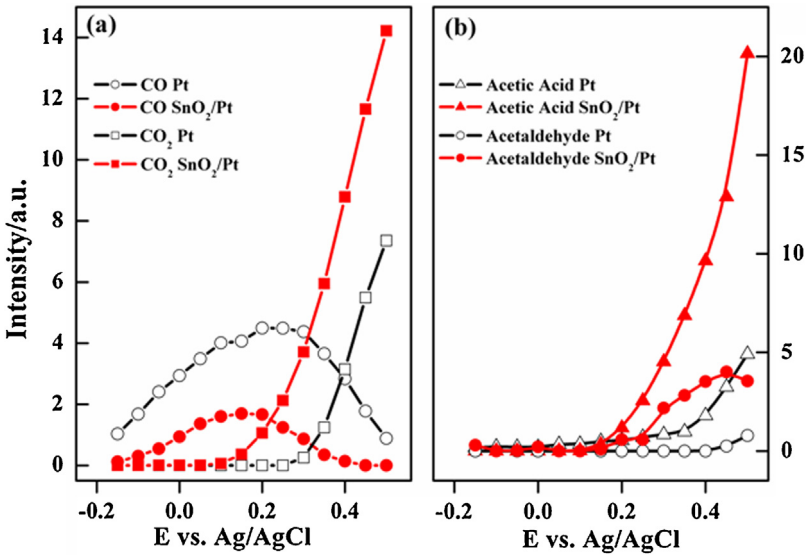

Fig. 5. Integrated band intensities as a function of applied potential for both the bare pc-Pt and SnO_2/Pt electrodes: (a) CO_2 and linear-bound CO_{ads}; (b) acetic acid and acetaldehyde.

acid formation due to a decrease in the available Pt active sites for C–C bond splitting. We expect the polycrystalline Pt surface used in this work to have a large number of steps and other defect sites (*e.g.* grain boundaries) which could act as active sites for C–C bond splitting such as those found for highly stepped surfaces. In this work, however, SnO_2 nanoparticles are randomly deposited on the pc-Pt surface and not selectively at steps as in the work of Del Colle et al. [26]. Hence, some defect sites will clearly be blocked, which will decrease the effectiveness of C–C bond splitting, but deposition will also occur on the terraces, presumably where acetic acid and acetaldehyde are preferentially formed. Despite having fewer active sites exposed on the SnO_2 covered pc-Pt surface, the results in Fig. 5a and b show that the yields of both the total (CO_2) partial oxidation (acetaldehyde and acetic acid) products are enhanced. Further improvement of the catalytic selectivity of SnO_2/Pt catalysts may be achieved by optimizing the SnO_2/Pt surface, for example, by strategically depositing SnO_2 at Pt terrace sites to block the acetic acid formation pathway while keeping the low-coordination Pt sites for C–C bond splitting. Alternatively, the catalytic efficiency of SnO_2/Pt may be improved by adding a third element to the catalyst surface, such as Rh, that is more effective for C–C bond splitting [14,16]. Ongoing studies in this area involve investigating the mechanism of EOR on well-defined, UHV prepared SnO_2/Pt electrocatalysts, including the addition of a second metal to enhance C–C bond splitting and selectivity.

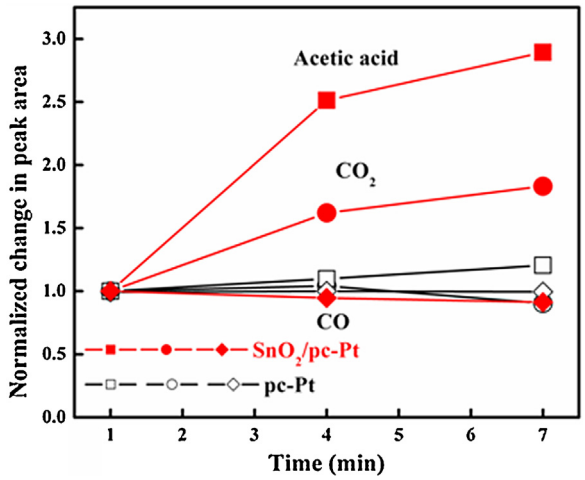

Fig. 6. Normalized band intensities of linear-bound CO_{ads}, CO_2, and acetic acid (1280 cm^{-1}) under a constant polarization of 0.2 V over time. The band intensities for all three species at a given reaction time were normalized to the one recorded after 1 min of polarization. This normalization provides a better visual description of product evolution with reaction time.

4. Conclusions

The present study of a pc-Pt-supported SnO_2 NP system clearly demonstrates the catalytic effect of SnO_2 nanoparticles in promoting the electrooxidation of ethanol and provides new insight into the reaction mechanism on SnO_2/Pt binary catalyst surfaces. The enhanced electrochemical activity of SnO_2/pc-Pt electrodes for the EOR is evidenced by a negatively shifted onset potential of ~0.17 V and a 10-fold increase in current density at low potentials (0.2 V). Our study suggests that the enhanced activity is directly linked to the catalytic function of SnO_2 co-catalysts, which provides OH species for the effective oxidative removal of surface CO_{ads}. Moreover, *in situ* IRRAS results also suggest that the presence of OH species provided by the SnO_2 NPs does not affect the C–C bond splitting ability of Pt active sites, which is also a key step for the complete conversion of ethanol to CO_2. The enhanced oxidation capabilities of small SnO_2 NPs on Pt also leads to increased production partial oxidation products acetaldehyde and acetic acid, which lowers the overall selectivity and efficiency.

Acknowledgments

This work carried out at Brookhaven National Laboratory was supported by U.S Department of Energy, Office of Basic Energy Sciences, Divisions of Chemical Sciences, under Contract No. DE-AC02-98CH10886. TEM images were obtained by Dong Su at the Center for Functional Nanomaterials at Brookhaven National Laboratory.

References

[1] C. Lamy, E.M. Belgsir, J.M. Leger, Journal of Applied Electrochemistry 31 (2001) 799–809.
[2] R.B. Kutz, B. Braunschweig, P. Mukherjee, R.L. Behrens, D.D. Dlott, A. Wieckowski, Journal of Catalysis 278 (2011) 181–188.

[3] M.T.M. Koper, S.C.S. Lai, E. Herrero, Electrocatalysis for the direct alcohol fuel cell, in: M.T.M. Koper (Ed.), Fuel Cell Catalysis: A Surface Science Approach, John Wiley & Sons, Inc., Hoboken, NJ, 2009.
[4] F. Colmati, G. Tremiliosi-Filho, E.R. Gonzalez, A. Berna, E. Herrero, J.M. Feliu, Physical Chemistry Chemical Physics 11 (2009) 9114–9123.
[5] S.C. Chang, L.W.H. Leung, M.J. Weaver, Journal of Physical Chemistry 94 (1990) 6013–6021.
[6] D.J. Tarnowski, C. Korzeniewski, Journal of Physical Chemistry B 101 (1997) 253–258.
[7] M.H. Shao, R.R. Adzic, Electrochimica Acta 50 (2005) 2415–2422.
[8] T. Iwasita, E. Pastor, Electrochimica Acta 39 (1994) 531–537.
[9] M. Heinen, Z. Jusys, R.J. Behm, Journal of Physical Chemistry C 114 (2010) 9850–9864.
[10] R. Kavanagh, X.M. Cao, W.F. Lin, C. Hardacre, P. Hu, Angewandte Chemie International Edition 51 (2012) 1572–1575.
[11] L. Jiang, G. Sun, Z. Zhou, S. Sun, Q. Wang, S. Yan, H. Li, J. Tian, J. Guo, B. Zhou, Q. Xin, Journal of Physical Chemistry B 109 (2005) 8774–8778.
[12] J. Mann, N. Yao, A.B. Bocarsly, Langmuir 22 (2006) 10432–10436.
[13] L. Jiang, L. Colmenares, Z. Jusys, G.Q. Sun, R.J. Behm, Electrochimica Acta 53 (2007) 377–389.
[14] A. Kowal, M. Li, M. Shao, K. Sasaki, M.B. Vukmirovic, J. Zhang, N.S. Marinkovic, P. Liu, A.I. Frenkel, R.R. Adzic, Nature Materials 8 (2009) 325–330.
[15] J.C.M. Silva, L.S. Parreira, R.F.B. De Souza, M.L. Calegaro, E.V. Spinace, A.O. Neto, M.C. Santos, Applied Catalysis B: Environmental 110 (2011) 141–147.
[16] M. Li, W.P. Zhou, N.S. Marinkovic, K. Sasaki, R.R. Adzic, Electrochimica Acta 104 (2013) 454–461.
[17] R. Alcala, J.W. Shabaker, G.W. Huber, M.A. Sanchez-Castillo, J.A. Dumesic, Journal of Physical Chemistry B 109 (2005) 2074–2085.
[18] F.J. Scott, S. Mukerjee, D.E. Ramaker, Journal of Physical Chemistry C 114 (2010) 442–453.
[19] E. Antolini, E.R. Gonzalez, Catalysis Today 160 (2011) 28–38.
[20] L. Colmenares, H. Wang, Z. Jusys, L. Jiang, S. Yan, G.Q. Sun, R.J. Behm, Electrochimica Acta 52 (2006) 221–233.
[21] M.Y. Zhu, G.Q. Sun, Q. Xin, Electrochimica Acta 54 (2009) 1511–1518.
[22] W.P. Zhou, W. An, D. Su, R. Palomino, P. Liu, M.G. White, R.R. Adzic, Journal of Physical Chemistry Letters 3 (2012) 3286–3290.
[23] W.P. Zhou, S. Axnanda, M.G. White, R.R. Adzic, J. Hrbek, Journal of Physical Chemistry C 115 (2011) 16467–16473.
[24] Y.E. Seidel, A. Schneider, Z. Jusys, B. Wickman, B. Kasemo, R.J. Behm, Faraday Discussions 140 (2009) 167–184.
[25] V. Del Colle, A. Berna, G. Tremiliosi-Filho, E. Herrero, J.M. Feliu, Physical Chemistry Chemical Physics 10 (2008) 3766–3773.
[26] V. Del Colle, J. Souza-Garcia, G. Tremiliosi-Filho, E. Herrero, J.M. Feliu, Physical Chemistry Chemical Physics 13 (2011) 12163–12172.
[27] R.B. Kutz, B. Braunschweig, P. Mukherjee, D.D. Dlott, A. Wieckowski, Journal of Physical Chemistry Letters 2 (2011) 2236–2240.